

Two-photon dilepton production in proton-proton collisions: two alternative approaches

Marta Łuszczak,^{1,*} Wolfgang Schäfer,^{2,†} and Antoni Szczurek^{3,‡}

¹*University of Rzeszów, PL-35-959 Rzeszów, Poland*

²*Institute of Nuclear Physics PAN, PL-31-342 Cracow, Poland*

³*Institute of Nuclear Physics PAN, PL-31-342 Cracow, Poland and
University of Rzeszów, PL-35-959 Rzeszów, Poland*

(Dated: July 3, 2021)

Abstract

We investigate different methods to incorporate the effect of photons in hard processes. We compare two different approaches used for calculating cross sections for two-photon $pp \rightarrow l^+l^-X$ process. In one of the approaches photon is treated as a collinear parton in the proton. In the second approach recently proposed a k_T -factorization method is used. We discuss how results of the collinear parton model depend on the initial condition for the QCD evolution and discuss an approximate treatment where photon is excluded from the combined QCD-QED evolution. We demonstrate that it is not necessary to put photon into the evolution equation as often done recently but it is sufficient to use a simplified approach in which photon couples to quarks and antiquarks which by themselves undergo DGLAP evolution equations. We discuss sensitivity of the results to the choice of structure function parametrization and experimental cuts in the k_T -factorization approach. A new optimal structure function parametrization is proposed. We compare results of our calculations with recent experimental data for dilepton production and find that in most cases the contribution of the photon-photon mechanism is rather small. We discuss how to enhance the photon-photon contribution. We also compare our results to those of recent measurements of exclusive and semi-exclusive e^+e^- pair production with certain experimental data by the CMS collaboration.

PACS numbers: 13.87.-a, 11.80La,12.38.Bx, 13.85.-t

*Electronic address: luszczak@univ.rzeszow.pl

†Electronic address: Wolfgang.Schafer@ifj.edu.pl

‡Electronic address: antoni.szczurek@ifj.edu.pl

I. INTRODUCTION

The two-photon processes may lead to production of two charged leptons and therefore compete with other sources of dileptons, such as continuum Drell-Yan processes or resonant production of vector quarkonia or Z^0 boson, which produce dilepton pairs of large invariant masses. Earlier studies of lepton pair production via $\gamma\gamma$ fusion in inelastic proton-proton collisions can be found in [1–4]. For a general review of the $\gamma\gamma$ -fusion mechanism, see [5]. Inelastic processes are also included in the Monte-Carlo generator LPAIR based on [6].

At high energies and small dilepton transverse momenta also semi-leptonic decays of pairwise produced charmed D mesons may be an important ingredient of dileptons [7]. Actual contribution of different processes depends strongly on the details of experimental cuts.

The color singlet exchange of photons naturally leads to rapidity gaps. If the rapidity veto on particles close to the l^+l^- vertex is imposed in addition one can enhance the relative contribution of the $\gamma\gamma$ processes compared to the QCD Drell-Yan mechanism [8]. The invariant mass distribution of dileptons produced in the Drell-Yan processes can be calculated in collinear-factorization approach (see e.g. the textbook [9]). If one wants to address more differential distributions, say in transverse momentum of the lepton pair, one can turn to b -space resummation [10] or, especially in the small- x kinematics, k_T -factorization (see [11–13] for instance).

In this paper we wish to concentrate on the photon-photon induced production of charged leptons. Realistic estimation of these processes requires more attention. In general, there are three types of such processes which can be classified according to whether the proton remnants appearing “after” photon emission are just protons or baryon resonances or a complicated continuum (see Fig.1). In principle, the elastic-elastic, processes with one elastic and one inelastic or double inelastic processes can be distinguished by detailed studies of the final state. However, in practice this separation may be not easy and all of them should be considered. Here we wish to concentrate rather on inelastic-inelastic processes.

There are two approaches in the literature in this context. In one of the approaches one can treat photons as collinear partons in the proton. The application of this approach requires presence of a hard scale (e.g. a large photon virtuality or large lepton transverse momenta). Such photon partonic distributions were discussed in [14–18]. In some of these approaches the photon PDF enters the DGLAP evolution equations. The treatment in [14] is somewhat simplified, here only the $q \rightarrow \gamma$ splitting is taken into account.

Below we wish to comment on the interrelation between the two approaches. The photon PDF approach was applied in many phenomenological studies, e.g. to a number of photon-photon processes in [19], and to dilepton production in [7].

In another approach one parametrizes the $\gamma^*p \rightarrow X$ vertices in terms of the proton’s structure functions. One can assume that the photons are either collinear or allow them to have transverse momenta and nonzero virtualities [5]. Recently we used a slightly simplified approach [4], which takes advantage of the high-energy limit and is formulated in an analogous way as the k_T -factorization approach often used in the context of two-gluon processes. In this approach one uses unintegrated photon distributions, in contrast to collinear distributions in the previous approach and off-shell matrix elements for the $\gamma\gamma \rightarrow l^+l^-$ subprocess. We shall use this approach also in the present paper.

The unintegrated photon distributions can be expressed in terms of the proton structure functions. The structure functions were measured in some different corners of very rich phase space. In particular they were studied in so-called deep-inelastic regime with large Q^2 where

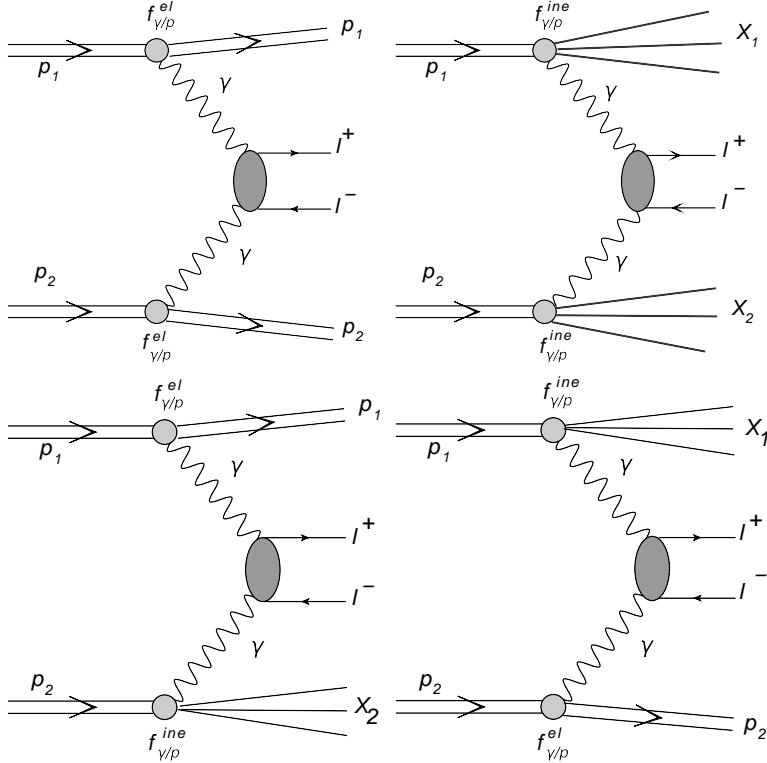


FIG. 1: Different mechanisms of two-photon production of dileptons.

perturbative treatment embedded in the DGLAP evolution equation applies. In this corner of the phase space the structure functions are very well known. When going outside of the perturbative regime the situation is less clear. Several parametrizations were presented in the literature [20–25]. The applicability of the different parametrizations is limited and not well tested.

Thus in two-photon processes one may need structure functions in very different corners of the (x, Q^2) space. It is not clear a priori which regions are needed for particular experiments i.e. specific kinematical cuts. We wish to discuss some examples related to particular past and modern experiments.

This paper is organized as follows: in section III, we briefly review the different formalism employed in our calculations. We also discuss the different structure functions used as an input in the k_T -factorization approach. In section IV we show our numerical results of various dilepton distributions for the kinematics, and cuts, relevant for different experiments. These are, at the presently highest available energies, ATLAS and CMS, which measure central rapidities, and LHCb with coverage at forward rapidities. We also discuss examples for the lower energies of RHIC, as well as data taken in 1980’s at the ISR at still lower energy. We summarize our results in Conclusions section.

II. COLLINEAR-FACTORIZATION APPROACH

A. Photons as partons in a hard process

Production of lepton pairs at large transverse momenta is a hard process, to which standard arguments for factorization apply, and collinear factorization should be an appropriate starting point to calculate e.g. rapidity or transverse momentum spectra of leptons. In fact, the dominant contribution to large-invariant mass dilepton pairs is of course the well known Drell-Yan process, but nothing prevents us from also including photon as partons along with quarks and gluons.

Then the photon parton distribution, $\gamma(z, Q^2)$, of photons carrying a fraction z of the proton's light-cone momentum, obeys the DGLAP equation,

$$\begin{aligned} \frac{d\gamma(z, Q^2)}{d \log Q^2} = & \frac{\alpha_{\text{em}}}{2\pi} \int_x^1 \frac{dy}{y} \left\{ \sum_f e_f^2 P_{\gamma \leftarrow q}(y) \left[q_f\left(\frac{z}{y}, Q^2\right) + \bar{q}_f\left(\frac{z}{y}, Q^2\right) \right] \right. \\ & \left. + P_{\gamma \leftarrow \gamma}(y) \gamma\left(\frac{z}{y}, Q^2\right) \right\}. \end{aligned} \quad (2.1)$$

In the complete set of DGLAP equations this photon density is then again coupled to the quark and antiquark distributions:

$$\begin{aligned} \frac{dq_f(z, Q^2)}{d \log Q^2} = & \frac{dq_f(z, Q^2)}{d \log Q^2} \Big|_{\text{QCD}} + \frac{\alpha_{\text{em}}}{2\pi} \int_x^1 \frac{dy}{y} \delta P_{q \leftarrow \gamma}^{\text{QED}}(y) q_f\left(\frac{z}{y}, Q^2\right) \\ & + \frac{\alpha_{\text{em}}}{2\pi} \int_x^1 \frac{dy}{y} P_{q \leftarrow \gamma}(y) \gamma\left(\frac{z}{y}, Q^2\right). \end{aligned} \quad (2.2)$$

Due to the smallness of α_{em} one would expect that the effect of photons on the quark and antiquark densities can be safely neglected, unless one is interested in high order perturbative corrections to the QCD splitting functions themselves.

Accordingly, we find two different approaches to DGLAP photons in the literature.

A first one, by Glück et al. [14] asserts, that we can neglect the photon density on the right hand side of the evolution equations. Then, at sufficiently large virtuality Q_0^2 , the photon parton density can be calculated from the collinear splitting of quarks and antiquarks $q \rightarrow q\gamma, \bar{q} \rightarrow \bar{q}\gamma$.

$$\frac{d\gamma(z, Q^2)}{d \log Q^2} = \frac{\alpha_{\text{em}}}{2\pi} \sum_f e_f^2 \int_z^1 \frac{dx}{x} P_{\gamma \leftarrow q}\left(\frac{z}{x}\right) \left[q_f(x, Q^2) + \bar{q}_f(x, Q^2) \right]. \quad (2.3)$$

This equation is easily integrated, and gives the photon parton density as

$$\begin{aligned} \gamma(z, Q^2) = & \sum_f \frac{\alpha_{\text{em}} e_f^2}{2\pi} \int_{Q_0^2}^{Q^2} \frac{d\mu^2}{\mu^2} \int_z^1 \frac{dx}{x} P_{\gamma \leftarrow q}\left(\frac{z}{x}\right) \left[q_f(x, \mu^2) + \bar{q}_f(x, \mu^2) \right] + \gamma(z, Q_0^2) \\ = & \frac{\alpha_{\text{em}}}{2\pi} \int_{Q_0^2}^{Q^2} \frac{d\mu^2}{\mu^2} \int_z^1 \frac{dx}{x} P_{\gamma \leftarrow q}\left(\frac{z}{x}\right) \frac{F_2(x, \mu^2)}{x} + \gamma(z, Q_0^2). \end{aligned} \quad (2.4)$$

One is left to specify – from some model considerations – the photon density at some low scale $\gamma(z, Q_0^2)$, but one may hope that at very large $Q^2 \gg Q_0^2 \sim 1 \text{ GeV}^2$ the part predicted perturbatively from quark and antiquark distributions dominates.

In addition to the above contribution from DGLAP splitting, Glück et al. also add the Weizsäcker-Williams flux from the coherent emission $p \rightarrow p\gamma^*$ without proton breakup as found in [5].

More recently, the Durham [15, 16] and NNPDF [17] groups have given a more involved treatment, in which the photon distribution is fully incorporated into the coupled DGLAP evolution equation. As usual with DGLAP evolution, the photon parton density at a starting scale $\gamma(z, Q_0^2)$ needs to be specified. While [15, 16] present model approaches, in Ref.[17] an ambitious attempt to obtain $\gamma(z, Q_0^2)$ from a fit to experimental data is found. Preliminary work by the CTEQ collaboration [18] is also based on QED corrected DGLAP equations, and attempts to fit the photon distribution from the prompt photon production $ep \rightarrow \gamma e X$ at HERA where in part of the phase space the Compton subprocess $e\gamma \rightarrow e\gamma$ contributes.

It should be noted, that in the approach of [15, 16], the input distribution $\gamma(z, Q_0^2)$ contains the coherent –or elastic– contribution with an intact proton in the final state. Notice that due to the proton form factors the integral over virtualities in the elastic case quickly converges, and the elastic contribution is basically independent of Q_0^2 , as soon as $Q_0^2 \gtrsim 0.7 \text{ GeV}^2$.

B. From photon PDFs to cross section

In the collinear approach the photon-photon contribution to inclusive cross section for dilepton production can be written as:

$$\frac{d\sigma^{(i,j)}}{dy_1 dy_2 d^2p_T} = \frac{1}{16\pi^2(x_1 x_2 s)^2} \sum_{i,j} x_1 \gamma^{(i)}(x_1, \mu^2) x_2 \gamma^{(j)}(x_2, \mu^2) \overline{|\mathcal{M}_{\gamma\gamma \rightarrow l+l^-}|^2}. \quad (2.5)$$

Here

$$\begin{aligned} x_1 &= \sqrt{\frac{p_T^2 + m_l^2}{s}} \left(\exp(y_1) + \exp(y_2) \right), \\ x_2 &= \sqrt{\frac{p_T^2 + m_l^2}{s}} \left(\exp(-y_1) + \exp(-y_2) \right). \end{aligned} \quad (2.6)$$

Above indices i and j denote $i, j = \text{el, in}$, i.e. they correspond to elastic or inelastic components similarly as for the k_T -factorization discussed in section III below, see also the diagrams in Fig.1. The factorization scale is chosen as $\mu^2 = m_T^2 = p_T^2 + m_l^2$.

The elastic photon distributions can be calculated with the help of elastic electromagnetic proton form factors. The functions $\gamma^{(\text{in})}(x, \mu^2)$ are precisely the DGLAP evolved distributions of section II A above.

C. Initial condition for collinear photon PDF

In the MRST2004(QED) approach the initial photon distribution is parametrized as [16]:

$$\gamma(z, Q_0^2) = \frac{\alpha_{\text{em}}}{2\pi} \int_z^1 \frac{dy}{y} \left[\frac{4}{9} \log\left(\frac{Q_0^2}{m_u^2}\right) u\left(\frac{z}{y}, Q_0^2\right) + \frac{1}{9} \log\left(\frac{Q_0^2}{m_d^2}\right) d\left(\frac{z}{y}, Q_0^2\right) \right] \cdot \frac{1 + (1-y)^2}{y}. \quad (2.7)$$

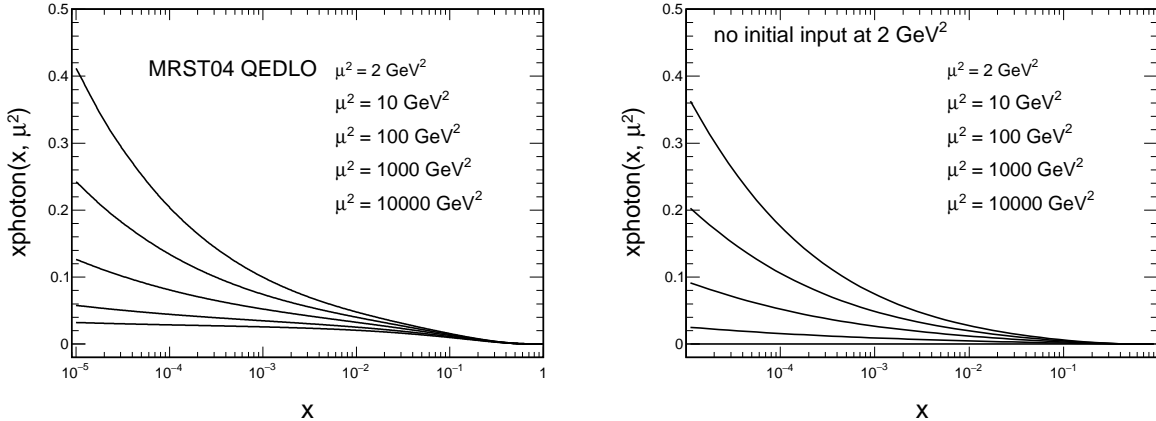


FIG. 2: Collinear photon distributions for different scales. The left panel is for standard MRST2004(QED) parton distribution, while the right panel is for the case when the initial input at $\mu^2 = 2 \text{ GeV}^2$ is set to zero, i.e. completely neglected.

Above $u(x, Q_0^2)$ and $d(x, Q_0^2)$ are valence-like distributions at the initial scale Q_0^2 . In actual calculation MRST2004(QED) uses current quark masses which causes that the $\log(\frac{Q_0^2}{m_q^2})$'s and in the consequence also the initial photon distributions are artificially large (the consequences for lepton production will be discussed when showing corresponding cross sections). It would seem more reasonable to use rather constituent quark masses than the current ones. We will show that this leads to large differences in photon distributions at finite running scales Q^2 .

Before discussing results for cross sections for l^+l^- production we wish to concentrate for a while on the collinear photon distributions. To illustrate the effect of the initial input in Fig.2 we show both original MRST2004(QED) photon distribution and similar result obtained by ignoring the initial input which, as discussed above, may be questionable. The results are shown for different evolution scales $\mu^2 = Q_0^2, 10, 100, 1000, 10000 \text{ GeV}^2$. We observe a sizable difference between resulting photon distributions obtained within the two approaches. Because in calculating the cross section the photon distributions enter twice in the cross section formula, for first and second proton, respectively, one can expect that the cross section obtained with the different PDFs may differ considerably. We will return to this issue in the Result section.

III. k_T -FACTORIZATION APPROACH

In this approach we start from the Feynman diagrams shown in Fig.1, and exploit the high-energy kinematics. Let the four-momenta of incoming protons be denoted p_A, p_B . At high energies the proton masses can be neglected, so that $p_A^2 = p_B^2 = 0$, $2(p_A \cdot p_B) = s$.

The photon-fusion production mechanism in leptonic and hadronic reactions is in great detail reviewed in [5], where also many original references can be found. In the most general form, the invariant cross section is written as a convolution of density matrices of photons in the beam particles, and helicity amplitudes for the $\gamma^*\gamma^* \rightarrow l^+l^-$ process. In a high energy limit, where dileptons carry only a small fraction of the total center-of-mass energy, the

density-matrix structure can be very much simplified, and there emerges a k_T -factorization representation of the cross section [4].

The unintegrated photon fluxes introduced in [4] can be expressed in terms of the hadronic tensor as

$$\mathcal{F}_{\gamma^* \leftarrow A}^{\text{in,el}}(z, \mathbf{q}) = \frac{\alpha_{\text{em}}}{\pi} (1-z) \left(\frac{\mathbf{q}^2}{\mathbf{q}^2 + z(M_X^2 - m_A^2) + z^2 m_A^2} \right)^2 \cdot \frac{p_B^\mu p_B^\nu}{s^2} W_{\mu\nu}^{\text{in,el}}(M_X^2, Q^2) dM_X^2. \quad (3.1)$$

These unintegrated fluxes enter the cross section for dilepton production as

$$\frac{d\sigma^{(i,j)}}{dy_1 dy_2 d^2\mathbf{p}_1 d^2\mathbf{p}_2} = \int \frac{d^2\mathbf{q}_1}{\pi\mathbf{q}_1^2} \frac{d^2\mathbf{q}_2}{\pi\mathbf{q}_2^2} \mathcal{F}_{\gamma^*/A}^{(i)}(x_1, \mathbf{q}_1) \mathcal{F}_{\gamma^*/B}^{(j)}(x_2, \mathbf{q}_2) \frac{d\sigma^*(p_1, p_2; \mathbf{q}_1, \mathbf{q}_2)}{dy_1 dy_2 d^2\mathbf{p}_1 d^2\mathbf{p}_2}, \quad (3.2)$$

where the indices $i, j \in \{\text{el, in}\}$ denote elastic or inelastic final states. The longitudinal momentum fractions of photons are obtained from the rapidities and transverse momenta of final state leptons as:

$$\begin{aligned} x_1 &= \sqrt{\frac{\mathbf{p}_1^2 + m_l^2}{s}} e^{y_1} + \sqrt{\frac{\mathbf{p}_2^2 + m_l^2}{s}} e^{y_2}, \\ x_2 &= \sqrt{\frac{\mathbf{p}_1^2 + m_l^2}{s}} e^{-y_1} + \sqrt{\frac{\mathbf{p}_2^2 + m_l^2}{s}} e^{-y_2}. \end{aligned} \quad (3.3)$$

The explicit form of the off-shell cross section $d\sigma^*(p_1, p_2; \mathbf{q}_1, \mathbf{q}_2)/dy_1 dy_2 d^2\mathbf{p}_1 d^2\mathbf{p}_2$ can be found in Ref. [4].

A. Inelastic vertices

We now first concentrate on inelastic processes with breakup of a proton. Then the hadronic tensor is expressed in terms of the electromagnetic currents as:

$$W_{\mu\nu}^{\text{in}}(M_X^2, Q^2) = \overline{\sum}_X (2\pi)^3 \delta^{(4)}(p_X - p_A - q) \langle p | J_\mu | X \rangle \langle X | J_\nu^\dagger | p \rangle d\Phi_X, \quad (3.4)$$

and its elements can be measured in inclusive electron scattering off the target. We wish to express it in terms of the virtual photoabsorption cross section of transverse and longitudinal photons. To this end we introduce the covariant vectors/tensors

$$e_\mu^{(0)} = \sqrt{\frac{Q^2}{X}} \left(p_{A\mu} - \frac{(p_A \cdot q)}{q^2} q_\mu \right), \quad X = (p_A \cdot q)^2 + m_A^2 Q^2, \quad e^{(0)} \cdot e^{(0)} = +1, \quad (3.5)$$

and

$$\delta_{\mu\nu}^\perp(p_A, q) = g_{\mu\nu} - \frac{q_\mu q_\nu}{q^2} - e_\mu^{(0)} e_\nu^{(0)}. \quad (3.6)$$

Here $\delta_{\mu\nu}^\perp$ projects on photons carrying helicity ± 1 in the γ^*p -cms frame, and $e_\mu^{(0)}$ plays the role of the polarization vector of the longitudinal photon. Notice that $q \cdot e^{(0)} = q^\mu \delta_{\mu\nu}^\perp = 0$, so that the hadronic tensor has the convenient gauge invariant decomposition

$$W_{\mu\nu}^{\text{in}}(M_X^2, Q^2) = -\delta_{\mu\nu}^\perp(p_A, q) W_T^{\text{in}}(M_X^2, Q^2) + e_\mu^{(0)} e_\nu^{(0)} W_L^{\text{in}}(M_X^2, Q^2). \quad (3.7)$$

The virtual photoabsorption cross sections are defined as

$$\begin{aligned}\sigma_T(\gamma^*p) &= \frac{4\pi\alpha_{\text{em}}}{4\sqrt{X}} \left(-\frac{\delta_{\mu\nu}^\perp}{2} \right) 2\pi W_{\mu\nu}^{\text{in}}(M_X^2, Q^2) \\ \sigma_L(\gamma^*p) &= \frac{4\pi\alpha_{\text{em}}}{4\sqrt{X}} e_\mu^0 e_\nu^0 2\pi W_{\mu\nu}^{\text{in}}(M_X^2, Q^2).\end{aligned}\quad (3.8)$$

It is customary to introduce dimensionless structure function $F_i(x_{\text{Bj}}, Q^2)$, $i = T, L$ as

$$\sigma_{T,L}(\gamma^*p) = \frac{4\pi^2\alpha_{\text{em}}}{Q^2} \frac{1}{\sqrt{1 + \frac{4x_{\text{Bj}}^2 m_A^2}{Q^2}}} F_{T,L}(x_{\text{Bj}}, Q^2), \quad (3.9)$$

where

$$x_{\text{Bj}} = \frac{Q^2}{Q^2 + M_X^2 - m_A^2}. \quad (3.10)$$

Then, our structure functions $W_{T,L}$ are expressed through the more conventional $F_{T,L}$ as

$$W_{T,L}^{\text{in}}(M_X^2, Q^2) = \frac{1}{x_{\text{Bj}}} F_{T,L}(x_{\text{Bj}}, Q^2). \quad (3.11)$$

In the literature one often finds rather $F_1(x_{\text{Bj}}, Q^2)$, $F_2(x_{\text{Bj}}, Q^2)$ structure functions, which are related to $F_{T,L}$ through

$$\begin{aligned}F_T(x_{\text{Bj}}, Q^2) &= 2x_{\text{Bj}}F_1(x_{\text{Bj}}, Q^2), \\ F_2(x_{\text{Bj}}, Q^2) &= \frac{F_T(x_{\text{Bj}}, Q^2) + F_L(x_{\text{Bj}}, Q^2)}{1 + \frac{4x_{\text{Bj}}^2 m_A^2}{Q^2}}.\end{aligned}\quad (3.12)$$

Now, performing the contraction with $p_B^\mu p_B^\nu$, we get

$$\frac{p_B^\mu p_B^\nu}{s^2} W_{\mu\nu}^{\text{in}}(M_X^2, Q^2) = \left(1 - \frac{z}{x_{\text{Bj}}} + \frac{z^2}{4x_{\text{Bj}}^2}\right) \frac{F_2(x_{\text{Bj}}, Q^2)}{Q^2 + M_X^2 - m_p^2} + \frac{z^2}{4x_{\text{Bj}}^2} \frac{2x_{\text{Bj}}F_1(x_{\text{Bj}}, Q^2)}{Q^2 + M_X^2 - m_p^2}. \quad (3.13)$$

In the deep inelastic region $F_2 \sim F_T + F_L$, and using $2x_{\text{Bj}}F_1 \sim F_2$ in the second term, we can write more succinctly

$$\frac{p_B^\mu p_B^\nu}{s^2} W_{\mu\nu}^{\text{in}}(M_X^2, Q^2) = Q^2 \cdot f_T\left(\frac{z}{x_{\text{Bj}}}\right) x_{\text{Bj}} F_2(x_{\text{Bj}}, Q^2), \quad (3.14)$$

with

$$f_T(y) = 1 - y + y^2/2 = \frac{1}{2} \left[1 + (1 - y)^2 \right]. \quad (3.15)$$

B. Elastic vertices

Let us now isolate the elastic contribution to the hadronic tensor, which we need to describe the photon flux in processes in which the proton stays intact. In this case, the structure functions $W_{T,L}$ are most conveniently written in terms of the electric and magnetic form factors $G_E(Q^2)$ and $G_M(Q^2)$ of the proton:

$$W_T^{\text{el}}(M_X^2, Q^2) = \delta(M_X^2 - m_p^2) Q^2 G_M^2(Q^2), \quad W_L^{\text{el}}(M_X^2, Q^2) = \delta(M_X^2 - m_p^2) 4m_p^2 G_E^2(Q^2) \quad (3.16)$$

The contribution to the photon flux is then again obtained by contracting

$$\frac{p_{Bj}^\mu p_{Bj}^\nu}{s^2} W_{\mu\nu}^{\text{el}}(M_X^2, Q^2) = \delta(M_X^2 - m_p^2) \left[\left(1 - \frac{z}{2}\right)^2 \frac{4m_p^2 G_E^2(Q^2) + Q^2 G_M^2(Q^2)}{4m_p^2 + Q^2} + \frac{z^2}{4} G_M^2(Q^2) \right] \quad (3.17)$$

C. Unintegrated photon fluxes

Let us now give explicit formulas for the unintegrated fluxes in a form which makes it easy to compare them for example with fluxes of virtual photons given by Budnev et al. [5]. The quantity to compare is the differential equivalent photon spectrum

$$dn^{\text{in,el}} = \frac{dz d^2\mathbf{q}}{z \pi \mathbf{q}^2} \mathcal{F}_{\gamma^* \leftarrow A}^{\text{in,el}}(z, \mathbf{q}). \quad (3.18)$$

The fluxes in [5] are given differentially in the virtuality Q^2 , instead of the transverse momentum $\mathbf{q}^2 = (1-z)(Q^2 - Q_{\text{min}}^2)$. We therefore substitute

$$\frac{d^2\mathbf{q}}{\pi \mathbf{q}^2} \rightarrow (1-z) \frac{dQ^2}{Q^2} \cdot \frac{Q^2}{\mathbf{q}^2} = \frac{dQ^2}{Q^2} \cdot \frac{Q^2}{Q^2 - Q_{\text{min}}^2} \quad \text{and} \quad \frac{\mathbf{q}^2}{\mathbf{q}^2 + z(M_X^2 - m_A^2) + z^2 m_A^2} = \frac{Q^2 - Q_{\text{min}}^2}{Q^2}, \quad (3.19)$$

so that we obtain

$$dn^{\text{in}} = \frac{\alpha_{\text{em}}}{\pi} \frac{dQ^2}{Q^2} \frac{dz}{z} (1-z) \left(1 - \frac{Q_{\text{min}}^2}{Q^2}\right) \times \left[\left(1 - \frac{z}{x_{\text{Bj}}} + \frac{z^2}{4x_{\text{Bj}}^2}\right) \frac{F_2(x_{\text{Bj}}, Q^2)}{Q^2 + M_X^2 - m_p^2} + \frac{z^2}{4x_{\text{Bj}}^2} \frac{2x_{\text{Bj}} F_1(x_{\text{Bj}}, Q^2)}{Q^2 + M_X^2 - m_p^2} \right] dM_X^2 \quad (3.20)$$

and for the elastic piece

$$dn^{\text{el}} = \frac{\alpha_{\text{em}}}{\pi} \frac{dQ^2}{Q^2} \frac{dz}{z} (1-z) \left(1 - \frac{Q_{\text{min}}^2}{Q^2}\right) \left[\left(1 - \frac{z}{2}\right)^2 \frac{4m_p^2 G_E^2(Q^2) + Q^2 G_M^2(Q^2)}{4m_p^2 + Q^2} + \frac{z^2}{4} G_M^2(Q^2) \right]. \quad (3.21)$$

It is also interesting to convert the integration over M_X^2 into one over x_{Bj} . To this end, we note that

$$\frac{dM_X^2}{Q^2 + M_X^2 - m_p^2} \rightarrow \frac{dx_{\text{Bj}}}{x_{\text{Bj}}}, \quad x_{\text{min}} = \frac{z}{1 - z^2 \frac{m_p^2}{Q^2}}, \quad x_{\text{max}} = \frac{Q^2}{Q^2 + (2m_p + m_\pi)m_\pi}. \quad (3.22)$$

Furthermore

$$(1-z)\left(1 - \frac{Q_{\min}^2}{Q^2}\right) = \frac{z}{x_{\text{Bj}}}\left(\frac{x_{\text{Bj}}}{x_{\min}} - 1\right) = 1 - \frac{z}{x_{\text{Bj}}} - \frac{z^2 m_p^2}{Q^2}. \quad (3.23)$$

Then we obtain for the photon flux

$$\begin{aligned} \frac{z dn^{\text{in}}(z, Q^2)}{dz d \log Q^2} &= \frac{\alpha_{\text{em}}}{\pi} \int_{x_{\min}}^{x_{\max}} \frac{dx_{\text{Bj}}}{x_{\text{Bj}}} \left(1 - \frac{z}{x_{\text{Bj}}} - \frac{z^2 m_p^2}{Q^2}\right) \left[\left(1 - \frac{z}{x_{\text{Bj}}} + \frac{z^2}{4x_{\text{Bj}}^2}\right) F_2(x_{\text{Bj}}, Q^2) \right. \\ &\quad \left. + \frac{z^2}{4x_{\text{Bj}}^2} 2x_{\text{Bj}} F_1(x_{\text{Bj}}, Q^2)\right]. \end{aligned} \quad (3.24)$$

In the deep inelastic limit, $x_{\min} \rightarrow z$, $x_{\max} \rightarrow 1$, and assuming $F_2 = 2x_{\text{Bj}} F_1$, this obtains the form

$$\frac{dn^{\text{in}}(z, Q^2)}{dz d \log Q^2} = \frac{\alpha_{\text{em}}}{2\pi} \int_z^1 \frac{dx_{\text{Bj}}}{x_{\text{Bj}}} P_{\gamma \leftarrow q}\left(\frac{z}{x_{\text{Bj}}}\right) \frac{F_2(x_{\text{Bj}}, Q^2)}{x_{\text{Bj}}} \left(1 - \frac{z}{x_{\text{Bj}}}\right), \quad (3.25)$$

with the splitting function

$$P_{\gamma \leftarrow q}(y) = \frac{1 + (1-y)^2}{y}. \quad (3.26)$$

The ‘‘parton densities of photons’’, which can be compared to the collinear factorization fluxes are

$$\gamma^{\text{in,el}}(z, \mu^2) = \int^{\mu^2} \frac{dQ^2}{Q^2} \frac{dn^{\text{in,el}}(z, Q^2)}{dz d \log Q^2}. \quad (3.27)$$

D. Structure functions as input for unintegrated fluxes

Here we show a few different parametrizations of the proton structure function F_2 . The different parametrizations taken from the literature are labeled as:

- ALLM [20, 21]. This parametrization gives a very good fit to F_2 in most of the measured region.
- FJLLM [22]. This parametrization explicitly includes the nucleon resonances and gives an excellent fit of the CLAS data.
- BDH [23]. This parametrization concentrates on the low- x , or high mass region. It features a Froissart-like behaviour at very small x .
- SY [24]. This parametrization of Suri and Yennie from the early 1970’s does not include QCD-DGLAP evolution. It is still today often used as one of the defaults in the LPAIR event generator.
- SU [25]. A parametrization which concentrates to give a good description at smallish and intermediate Q^2 at not too small x .

We also show F_2 calculated from the CTEQ6L parametrization [26].

In Fig.3 we show the proton structure function $F_2(x, Q^2)$ obtained from the various fits at $Q^2 = 0.225, 1.25, 2.5, 4.5 \text{ GeV}^2$ as a function of Bjorken- x in Fig. 3. In Fig. 4, we show the structure function $F_2(x, Q^2)$ at $Q^2 = 2.5 \text{ GeV}^2$, but this time with a logarithmic abscissa to emphasize the low- x behaviour of different parametrizations. Also shown are the HERA data at low- x . Experimental data on the figures are taken from the compilation [27] and from [28, 29].

Here we see that the Suri-Yennie fit corresponds to a unit-intercept Pomeron and does not describe the small- x rise of the proton structure function.

A surprising lesson is, that the old Suri-Yennie [24] fit, still gives a reasonable description of F_2 except of very small x .

For explicit account of resonances it would be recommended to use the Fiore et al. [22], but care has to be taken to stay within the resonance region, as the quality of the fit beyond this region quickly deteriorates.

The overall best description appears to be given by the ALLM [20, 21] fit.

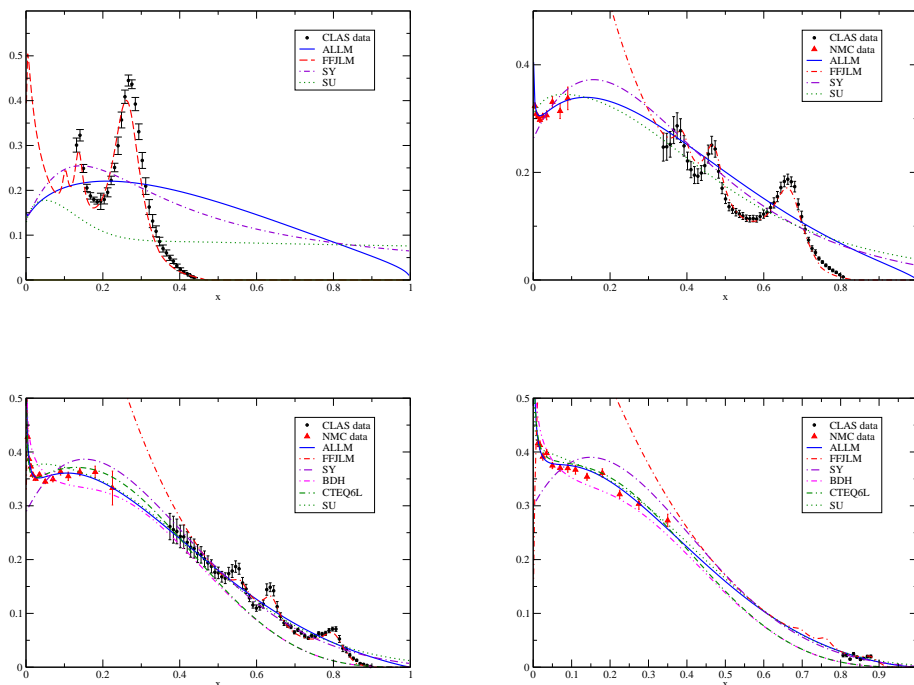


FIG. 3: The proton structure function $F_2(x, Q^2)$ as a function of x for $Q^2 = 0.225 \text{ GeV}^2$ (top left), $Q^2 = 1.25 \text{ GeV}^2$ (top right), $Q^2 = 2.5 \text{ GeV}^2$ (bottom left), and $Q^2 = 4.5 \text{ GeV}^2$ (bottom right). Shown are different parametrizations available in the literature.

E. Monte Carlo generator

In contrast to our previous studies [4], all calculations performed within the k_T -factorization approach were performed with a Monte Carlo event generator, where the

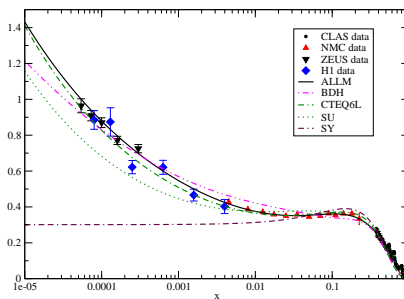


FIG. 4: The proton structure function $F_2(x, Q^2)$ as a function of x at $Q^2 = 2.5 \text{ GeV}^2$, shown with a logarithmic x -axis, to make visible the small- x behaviour of different parametrizations. Here also HERA data are included.

formulae presented above (see also [4]) were implemented. This Monte Carlo program is used to generate events (four-momenta of leptons and outgoing protons/excited systems) which are then transformed to distributions with the help of the standard software Root [31]. The typical number of events generated in our studies is a few millions. A more detailed description of the event generator will be presented elsewhere [30].

IV. RESULTS

Most of the experiments for the dilepton production concentrate on determination of dilepton invariant mass distributions. In Fig.5 we show invariant mass distributions of dilepton pairs produced in the photon-photon inelastic-inelastic mechanism for kinematical conditions relevant for different experiments. We show results obtained with different parametrizations of the structure functions known from the literature. Surprisingly the different structure functions give quite different results. For completeness in some cases (when possible) we also show the result obtained in the collinear approach with the MRST2004(QED) photon distribution with (solid black line) and similar one when ignoring the initial input (long-dashed black line). The result obtained within the collinear approach with the MRST2004(QED) distribution is much above the results obtained within the k_T -factorization approach. In our opinion this is mainly related to the large input photon distribution at the initial scale $Q_0^2 = 2 \text{ GeV}^2$ (see Eq.(2.7)) discussed in the context of Fig.2. If the input is discarded (long-dashed black line) the collinear result is similar to the results obtained within the k_T -factorization. The inelastic-inelastic contribution gives only a small fraction of the measured cross section for most experimental conditions (ATLAS,LHCb,PHENIX). For the ISR experiment it is relatively larger.

In Fig.6 we show dilepton invariant mass distributions for elastic-inelastic and inelastic-elastic (added together) contributions. As for inelastic-inelastic contribution the results strongly depend on the parametrization of the structure functions used. The spread of results for different F_2 from the literature is now, however, significantly smaller than in the case of inelastic-inelastic contributions where the structure functions enter twice (into both photon flux factors). As for the double inelastic case we also show a result for the collinear approach. The mixed components give similar contribution to the dilepton invariant mass

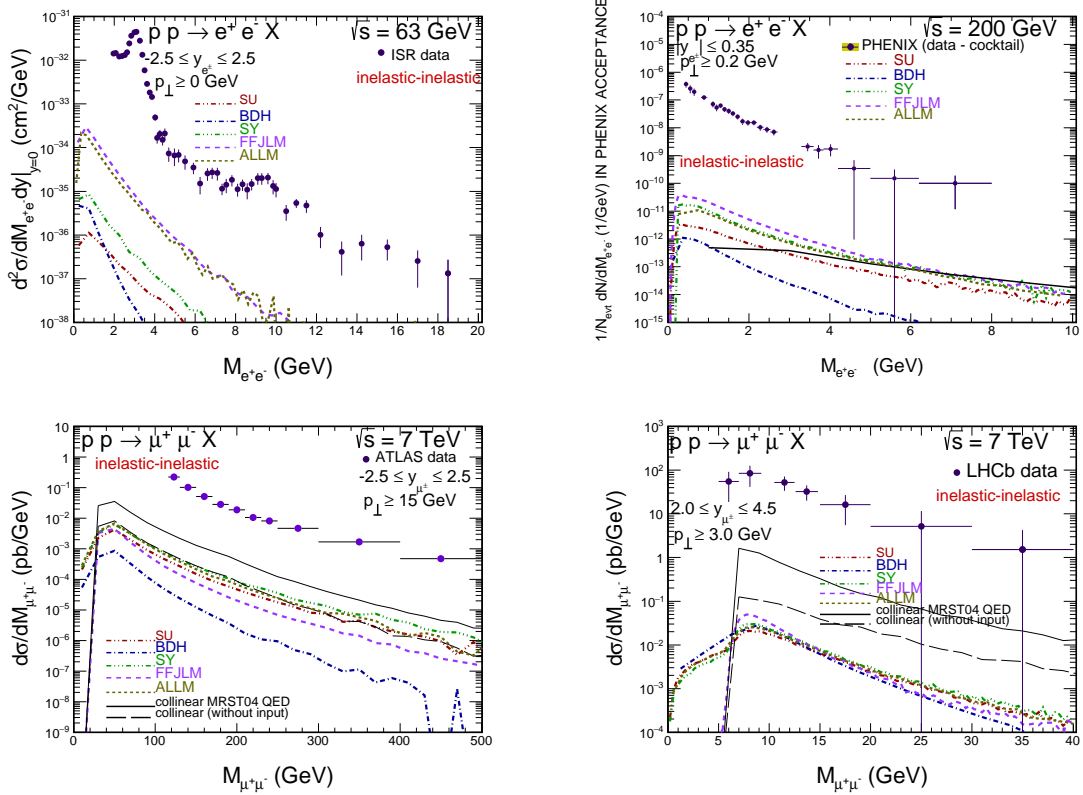


FIG. 5: The inelastic-inelastic contribution to dilepton invariant mass distributions for the ISR (upper-left), PHENIX (upper-right), ATLAS (lower-left) and LHCb (lower-right) experiments for different structure functions.

distributions as the inelastic-inelastic one.

It is very interesting to understand which regions of (Q_1^2, M_X) and (Q_2^2, M_Y) space contribute in the measured spectra. We start our review from distributions in M_X (or M_Y). The corresponding results for the inelastic-inelastic component are shown in Fig.7. Again we show results for the ISR (left top panel), PHENIX (right top panel) ATLAS (left bottom panel) and LHCb (right bottom panel) experiment. The dominant contributions come from the region of very small missing masses M_X (or M_Y). This is not necessarily the region where standard evolution equation applies for the description of F_2 structure function. In general, the Fiore et al. [22] and Suri-Yennie [24] parametrization give much bigger cross section in the region of small missing masses. In this plot the resolution in missing mass is rather coarse ($\Delta M_X = 2.5$ GeV). If the resolution of the distribution (binning) was improved one could observe even peaks corresponding to nucleon resonances excited by virtual photons for the Fiore et al. parametrization. As seen in Fig.3 the Suri-Yennie parametrization extremely well averages the structures in more detailed Fiore et al. parametrization. Clearly the Fiore et al. parametrization is not adequate for large M_X (M_Y) masses. All this demonstrates how important is using a “proper” structure function.

In Fig.8 we show some examples of two-dimensional distributions (M_X, M_Y) for different parametrizations of the structure functions as an example for the PHENIX kinematics. Here we focus on small values of M_X and M_Y to resolve apparent differences. Clearly the different parametrizations give very different results. In the case of Fiore et al. parametrization one

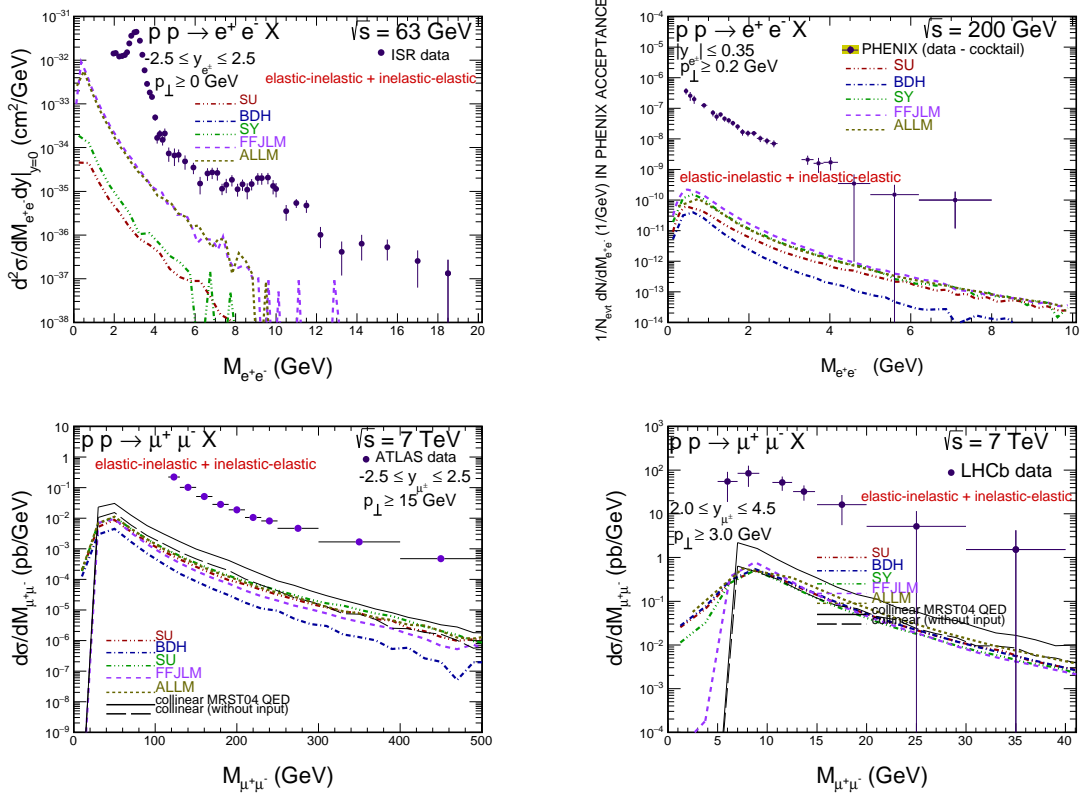


FIG. 6: The (elastic-inelastic)+(inelastic-elastic) contribution to dilepton invariant mass distributions for the ISR (upper-left), PHENIX (upper-right), ATLAS (lower-left) and LHCb (lower-right) experiments for different structure functions.

can observe now (with better resolution) resonance lines for M_X or M_Y slightly bigger than 1 GeV.

In Fig.9 we show two-dimensional distributions (Q_1^2, Q_2^2) for four different experimental conditions specified in the figure caption. In most of the cases rather large photon virtualities contribute. This is especially true for the ATLAS experiment with large cuts on lepton transverse momenta [36]. In the case of the old ISR experiment [38] or more recent PHENIX experiment [33] the situation is very different and clearly contributions from F_2 nonperturbative regions come into game and should be carefully analyzed. For the case of LHCb, in contrast to other cases, the distribution in $Q_1^2 \times Q_2^2$ is not symmetric along the diagonal which is related to asymmetric forward coverage of the LHCb experiment.

Summarizing this part, we have shown that with typical experimental cuts the contribution of photon-photon fusion is much smaller than dilepton experimental data and constitutes typically less than 1 % of the measured cross sections.

In most of the cases considered so far Drell-Yan processes dominate [12, 13]. However, the two-photon processes are interesting by themselves. Can they be measured experimentally? In order to reduce the Drell-Yan contribution and relatively enhance the two-photon contribution one can impose an extra condition on lepton isolation. First trials have been already done by the CMS collaboration [8]. In their analysis an extra lepton isolation cuts were imposed in order to eliminate the otherwise dominating Drell-Yan component. In Figs. 10,11,12 we show our results for two different (SY and ALLM) parametrizations of the struc-

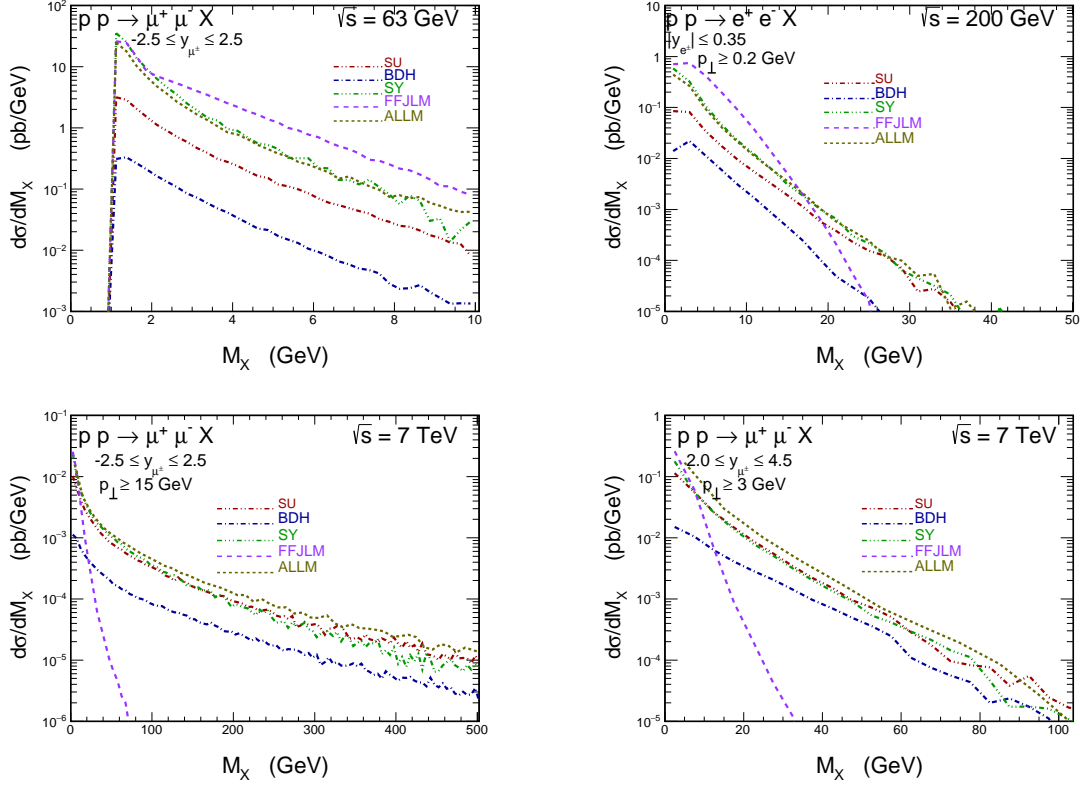


FIG. 7: Missing mass distributions for inelastic-inelastic photon-photon contributions for different experiments (ISR, PHENIX, ATLAS, LHCb) and different parametrizations of the structure functions as explained inside the figures.

ture functions for distributions in dimuon invariant mass, in transverse momentum of the pair and in relative azimuthal angle between $\mu^+\mu^-$. Only invariant mass distribution can be obtained in the collinear approach. In the collinear approach the second and the third distributions are just Dirac delta functions in $p_{T,pair}$ and $\phi_{\mu^+\mu^-}$, respectively. SY and ALLM parametrizations give almost the same contributions to all the distributions considered. In the first evaluation we have taken into account integrated luminosity of the experiment ($L = 63.2 \text{ pb}^{-1}$) as well as experimental acceptances given in Table 5 in Ref.[39]. Rather good agreement with the low statistics CMS experimental data is achieved (for both parametrizations of structure functions used in the figures) without including any extra corrections due to absorption effects leading to destroying the rapidity isolation of leptons and a damping of corresponding cross section for the photon-photon mechanisms. This result is interesting by itself. It may mean that the absorption effects are small or alternatively that a contamination of the Drell-Yan contribution is still not completely removed. Both effects should be therefore studied in more detail in a future. This can be done by full Monte Carlo simulations of both processes and clearly goes beyond the scope of the present analysis.

For completeness and comparison in Fig.13 we show invariant mass distribution obtained within collinear factorization approach with $\mu^2 = m_T^2$. We present results for the case when initial input at $Q_0^2 = \text{GeV}^2$ (see Eq.(2.7)) is included (thick red lines) as well as when it is discarded (thin blue lines) as discussed in subsection II A. The results obtained in the latter case are slightly larger than those obtained within the k_T -factorization approach (see

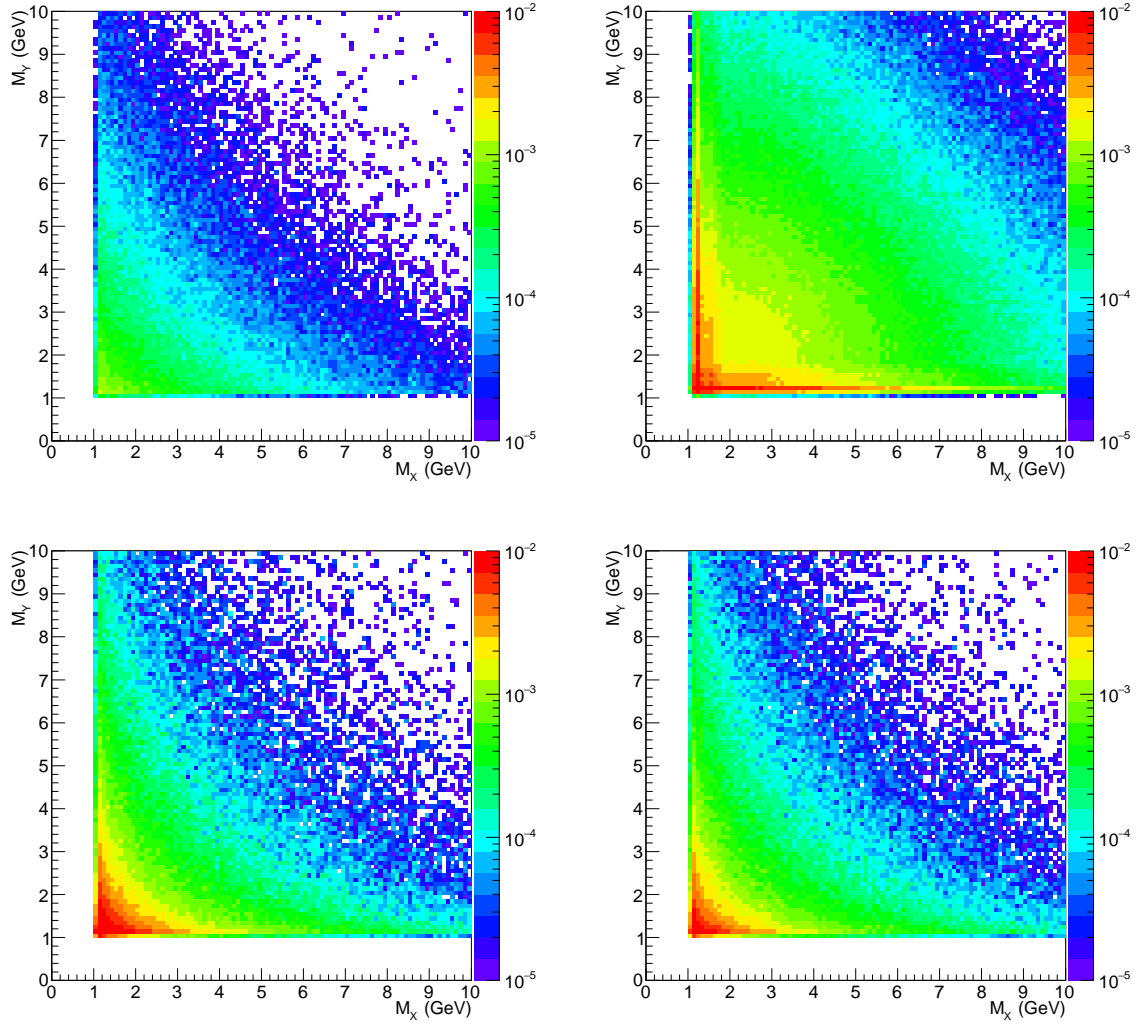


FIG. 8: Distributions for $M_X \times M_Y$ for different structure functions: Szczurek-Uleshchenko (upper-left), Fiore et al. (upper-right), Suri-Yennie (lower-right) and ALLM (lower-left) for $\sqrt{s} = 200$ GeV and $p_{T1}, p_{T2} > 0.2$ GeV.

Fig.10), especially when the MRST(QED) input is included.

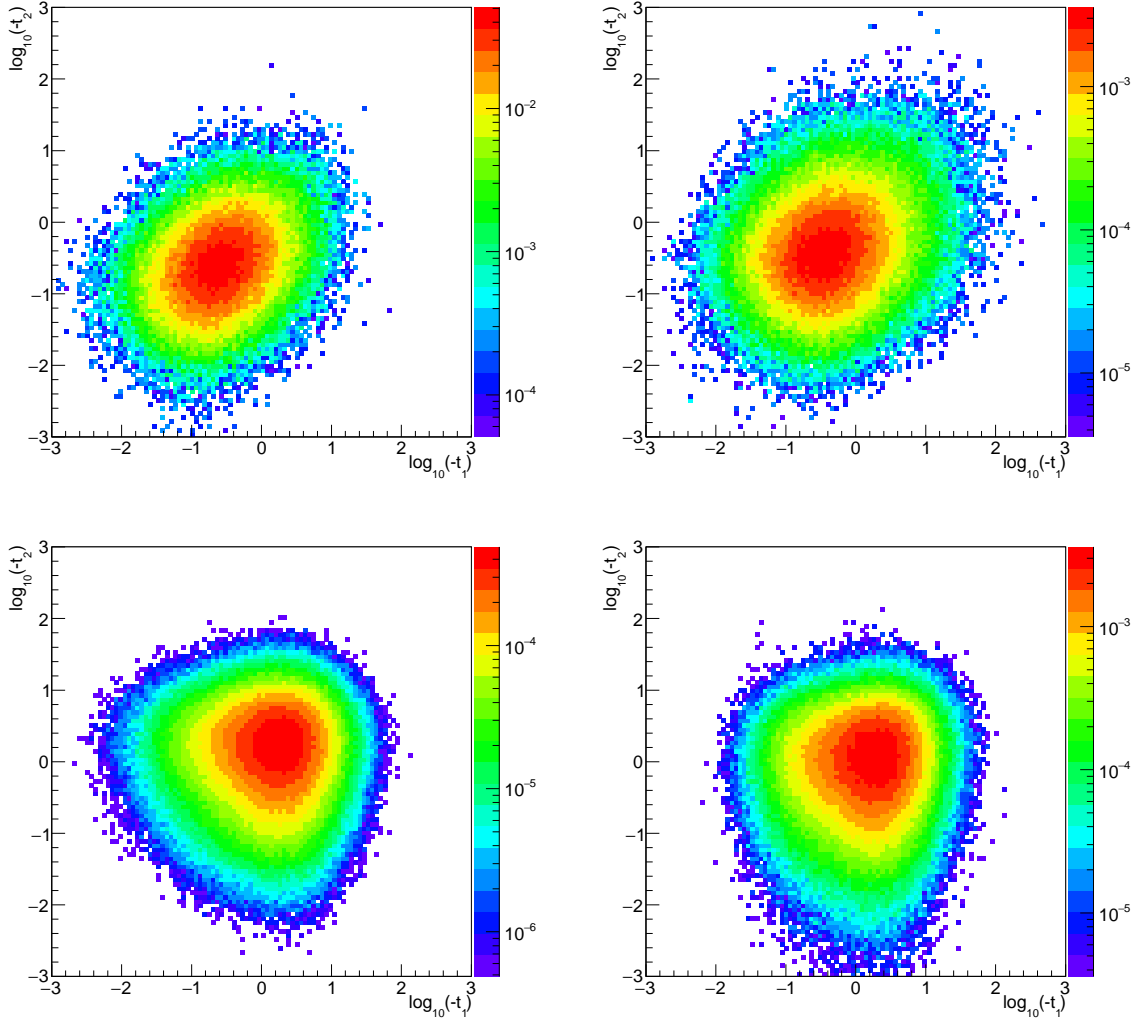


FIG. 9: Distributions for $Q_1^2 \times Q_2^2$ for different experiments: ISR (upper-left), PHENIX (upper-right), ATLAS (lower-right) and LHCb (lower-left) for ALLM structure function.

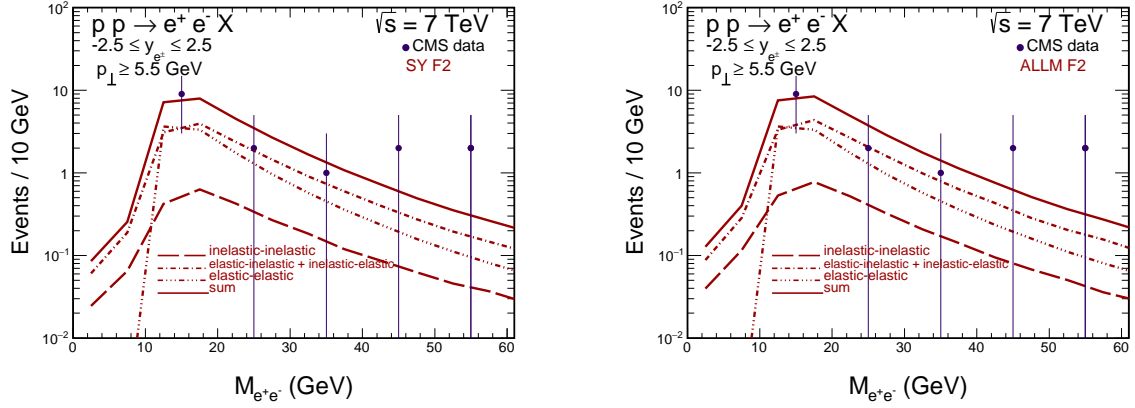


FIG. 10: Number of events per invariant mass interval for the CMS experimental cuts for SY (left) and ALLM (right) structure functions. The experimental data points are from Ref.[39].

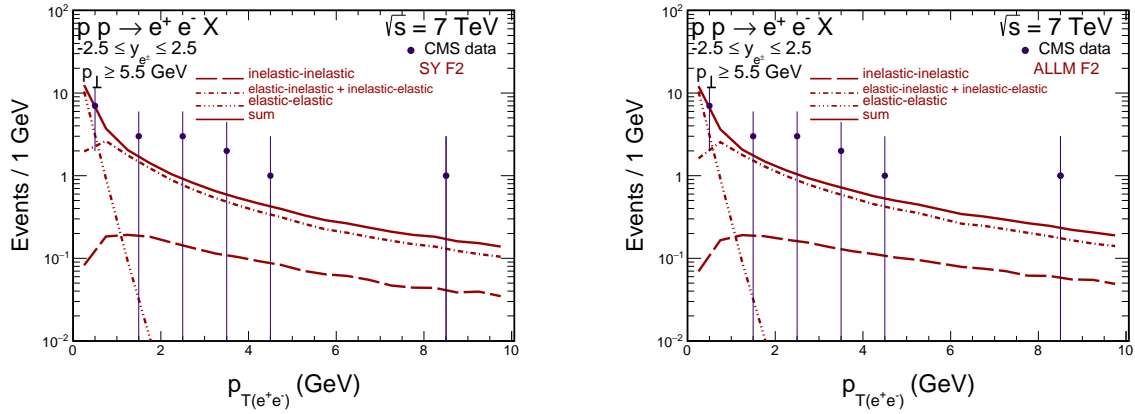


FIG. 11: Number of events per pair transverse momentum interval for the CMS experimental cuts for SY (left) and ALLM (right) structure functions. The experimental data points are from Ref.[39].

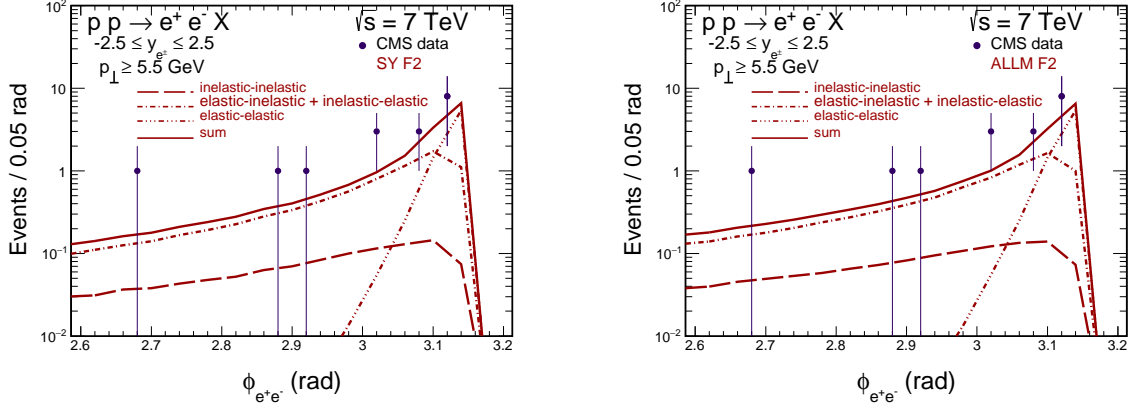


FIG. 12: Number of events per pair relative azimuthal angle interval for the CMS experimental cut for SY (left) and ALLM (right) structure functions. The experimental data points are from Ref.[39].

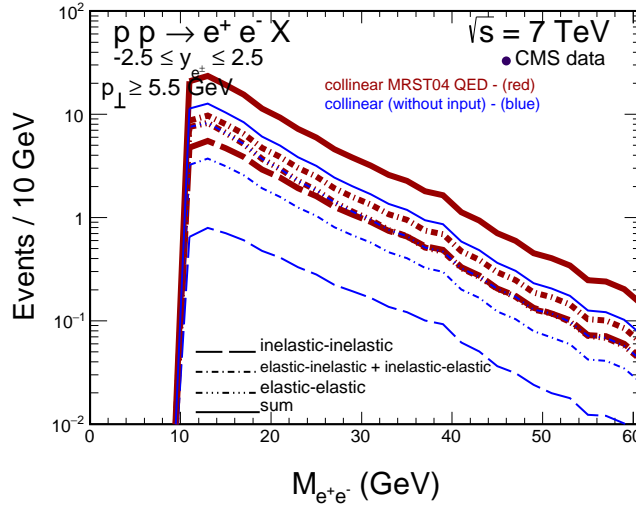


FIG. 13: Number of events per invariant mass interval for the CMS experimental cuts for collinear factorization approach. The results when initial MRST2004(QED) input is included (thick (red on line) lines) is compared with those when it is discarded (thin (blue on line) lines). The experimental data points are from Ref.[39].

V. CONCLUSIONS

In the present paper we have discussed in detail production of dilepton pairs (e^+e^- or $\mu^+\mu^-$) in photon-photon processes in proton-proton scattering at high energies. We have compared two different distinct theoretical approaches.

In the first approach photon is treated as a collinear parton in the proton and included into generalized (QCD,QED) DGLAP equations. We have discussed and demonstrated that it is not necessary to keep photon distribution in the evolution equation. It is sufficient to couple photon to other partons (quarks/antiquarks) in the proton, that undergo usual DGLAP evolution equations. We have discussed also the issue of initial condition for the photon distribution at the initial scale. In this context we have discussed parametrization/prescription proposed by MRST04(QED) [15] with their initial input as well as when starting evolution from zero input. The two prescriptions lead to quite different results for photon distributions and in the consequence also for charged lepton observables for finite scales.

In the second approach we take into account the fact that photons are off shell and include their transverse momenta and/or virtualities. We have shown that for typical kinematical conditions of modern experiments, especially at the LHC, the photon virtualities are fairly large, which puts doubts on the standard (collinear) parton model treatment. The k_T -factorization approach uses unintegrated photon distributions which are expressed in terms of F_2 structure functions [4]. Different model parametrizations known from the literature have been used in the present study. The final results depend strongly on the choice of the parametrization. We have identified regions of the (Q_i^2, M_i) space which give significant contribution to the cross section for different experimental conditions. For example for the experimental cuts of the recent ATLAS experiment [36] mostly perturbative region ($Q_i^2 > 4$ GeV and $W_i > 3$ GeV) contributes. Therefore a reliable predictions with accuracy better than 10 % are possible. In contrast, for the old ISR [38] and more recent PHENIX [33] experiments substantial contributions come from the regions $W_i < 3$ GeV and $Q_i^2 < 1$ GeV. In this case one should use explicit parametrizations which fit experimental data in this corner of the space. The calculation should take into account also resonance contributions.

In the present paper we have discussed production of dileptons. Similar analysis may be repeated e.g. for photon-photon induced production of W^+W^- pairs. So far only the first approach was applied there [19].

Acknowledgements

We would like to thank Juan Rojo for remarks that initiated the present study, and Laurent Forthomme for help with a Monte Carlo code. This study was partially supported by the Polish National Science Centre grants DEC-2013/09/D/ST2/03724 and DEC-2014/15/B/ST2/02528.

-
- [1] M. S. Chen, I. J. Muzinich, H. Terazawa and T. P. Cheng, "Lepton pair production from two-photon processes," *Phys. Rev. D* **7**, 3485 (1973).
 - [2] C. Carimalo, P. Kessler and J. Parisi, " $\gamma\gamma$ Background of the Drell-Yan Process," *Phys. Rev. D* **18** (1978) 2443 [*Phys. Rev. D* **19** (1979) 2233].

- [3] B. Schrempp and F. Schrempp, “Two Photon Exchange in $p(\bar{p}) \rightarrow \ell^+ \ell^- X$ and a Comparison With QCD,” Nucl. Phys. B **182** (1981) 343.
- [4] G. G. da Silveira, L. Forthomme, K. Piotrkowski, W. Schäfer and A. Szczurek, “Central $\mu^+ \mu^-$ production via photon-photon fusion in proton-proton collisions with proton dissociation,” JHEP **1502**, 159 (2015) [arXiv:1409.1541 [hep-ph]].
- [5] V. M. Budnev, I. F. Ginzburg, G. V. Meledin and V. G. Serbo, “The Two photon particle production mechanism. Physical problems. Applications. Equivalent photon approximation,” Phys. Rept. **15**, 181 (1975).
- [6] J. A. M. Vermaseren, “Two Photon Processes at Very High-Energies,” Nucl. Phys. B **229**, 347 (1983).
- [7] R. Maciuła, A. Szczurek and G. Ślipek, “Kinematical correlations of dielectrons from semileptonic decays of heavy mesons and Drell-Yan processes at BNL RHIC”, Phys. Rev. **D83** (2011) 054014.
- [8] S. Chatrchyan *et al.* [CMS Collaboration], “Search for exclusive or semi-exclusive photon pair production and observation of exclusive and semi-exclusive electron pair production in pp collisions at $\sqrt{s} = 7$ TeV,” JHEP **1211**, 080 (2012) [arXiv:1209.1666 [hep-ex]].
- [9] R. K. Ellis, W. J. Stirling and B. R. Webber, “QCD and collider physics,” Camb. Monogr. Part. Phys. Nucl. Phys. Cosmol. **8** (1996) 1.
- [10] J. C. Collins, D. E. Soper and G. F. Sterman, “Transverse Momentum Distribution in Drell-Yan Pair and W and Z Boson Production,” Nucl. Phys. B **250** (1985) 199.
- [11] A. Szczurek and G. Ślipek, “Parton transverse momenta and Drell-Yan dilepton production,” Phys. Rev. D **78** (2008) 114007 [arXiv:0808.1360 [hep-ph]].
- [12] M. A. Nefedov, N. N. Nikolaev and V. A. Saleev, “Drell-Yan lepton pair production at high energies in the Parton Reggeization Approach,” Phys. Rev. D **87** (2013) 1, 014022 [arXiv:1211.5539 [hep-ph]].
- [13] S. P. Baranov, A. V. Lipatov and N. P. Zotov, “Drell-Yan lepton pair production at the LHC and transverse momentum dependent quark densities of the proton,” Phys. Rev. D **89** (2014) 9, 094025 [arXiv:1402.5496 [hep-ph]].
- [14] M. Glück, C. Pisano and E. Reya, “The Polarized and unpolarized photon content of the nucleon,” Phys. Lett. B **540**, 75 (2002) [hep-ph/0206126].
- [15] A. D. Martin, R. G. Roberts, W. J. Stirling and R. S. Thorne, “Parton distributions incorporating QED contributions,” Eur. Phys. J. C **39**, 155 (2005) [hep-ph/0411040].
- [16] A. D. Martin and M. G. Ryskin, “The photon PDF of the proton,” Eur. Phys. J. C **74**, 3040 (2014) [arXiv:1406.2118 [hep-ph]].
- [17] R. D. Ball *et al.* [NNPDF Collaboration], “Parton distributions with QED corrections,” Nucl. Phys. B **877**, 290 (2013) [arXiv:1308.0598 [hep-ph]].
- [18] C. Schmidt, J. Pumplin, D. Stump and C.-P. Yuan, “QED effects and Photon PDF in the CTEQ-TEA Global Analysis,” PoS DIS **2014**, 054 (2014).
- [19] M. Luszczak, A. Szczurek and Ch. Royn, “ W^+W^- pair production in proton-proton collisions: small missing terms”, JHEP **02** (2015) 098.
- [20] H. Abramowicz, E. M. Levin, A. Levy and U. Maor, “A Parametrization of sigma-T (gamma* p) above the resonance region $Q^{*2} \geq 0$,” Phys. Lett. B **269** (1991) 465.
- [21] H. Abramowicz and A. Levy, “The ALLM parameterization of sigma(tot)(gamma* p): An Update,” hep-ph/9712415.
- [22] R. Fiore, A. Flachi, L. L. Jenkovszky, A. I. Lengyel and V. K. Magas, “Explicit model realizing parton hadron duality,” Eur. Phys. J. A **15**, 505 (2002) [hep-ph/0206027].

- [23] M. M. Block, L. Durand and P. Ha, “Connection of the virtual γ^*p cross section of ep deep inelastic scattering to real γp scattering, and the implications for νN and ep total cross sections,” *Phys. Rev. D* **89**, no. 9, 094027 (2014) [arXiv:1404.4530 [hep-ph]].
- [24] A. Suri and D. R. Yennie, “The Space-time Phenomenology Of Photon Absorption And Inelastic Electron Scattering,” *Annals Phys.* **72**, 243 (1972).
- [25] A. Szczurek and V. Uleshchenko, “Nonpartonic components in the nucleon structure functions at small Q^{*2} in the broad range of x ,” *Eur. Phys. J. C* **12**, 663 (2000) [hep-ph/9904288].
- [26] J. Pumplin, D. R. Stump, J. Huston, H. L. Lai, P. M. Nadolsky and W. K. Tung, “New generation of parton distributions with uncertainties from global QCD analysis,” *JHEP* **0207** (2002) 012 [hep-ph/0201195].
- [27] T. Gehrmann, R. G. Roberts and M. R. Whalley, “A compilation of structure functions in deep inelastic scattering,” *J. Phys. G* **25** (1999) A1.
- [28] M. Osipenko *et al.*, “The Proton structure function $F(2)$ with CLAS,” hep-ex/0309052.
- [29] M. Osipenko *et al.* [CLAS Collaboration], “A Kinematically complete measurement of the proton structure function $F(2)$ in the resonance region and evaluation of its moments,” *Phys. Rev. D* **67** (2003) 092001 [hep-ph/0301204].
- [30] L. Forthomme, K. Piotrkowski, G. da Silveira, W. Schäfer and A. Szczurek, to be published.
- [31] <https://root.cern.ch/>
- [32] G. Kubasiak and A. Szczurek, “Inclusive and exclusive diffractive production of dilepton pairs in proton-proton collisions at high energies”, *Phys. Rev.* **D84** (2011) 014005.
- [33] A. Adare *et al.* [PHENIX Collaboration], “Dilepton mass spectra in p+p collisions at $s^{*1/2} = 200$ -GeV and the contribution from open charm,” *Phys. Lett. B* **670** (2009) 313 [arXiv:0802.0050 [hep-ex]].
- [34] [The LHCb collaboration], “Inclusive low mass Drell-Yan production in the forward region at $\sqrt{s}=7$ TeV ,” LHCb-CONF-2012-013; Conference report prepared for XX International Workshop on Deep-Inelastic Scattering and Related Subjects, 26-30, March 2012, Bonn, Germany.
- [35] G. Aad *et al.* [ATLAS Collaboration], “Measurement of the low-mass Drell-Yan differential cross section at $\sqrt{s} = 7$ TeV using the ATLAS detector,” *JHEP* **1406**, 112 (2014) [arXiv:1404.1212 [hep-ex]].
- [36] G. Aad *et al.* [ATLAS Collaboration], “Measurement of the high-mass Drell-Yan differential cross-section in pp collisions at $\sqrt{s}=7$ TeV with the ATLAS detector,” *Phys. Lett. B* **725**, 223 (2013) [arXiv:1305.4192 [hep-ex]].
- [37] V. Khachatryan *et al.* [CMS Collaboration], “Measurements of differential and double-differential Drell-Yan cross sections in proton-proton collisions at 8 TeV,” *Eur. Phys. J. C* **75**, no. 4, 147 (2015) [arXiv:1412.1115 [hep-ex]].
- [38] C. Kourkoumelis, L. K. Resvanis, T. A. Filippas, E. Fokitis, A. M. Cnops, J. H. Cobb, R. Hogue and S. Iwata *et al.*, “Study of Massive Electron Pair Production at the CERN Intersecting Storage Rings,” *Phys. Lett. B* **91** (1980) 475.
- [39] S. Chatrchyan *et al.* [CMS Collaboration], “Search for exclusive or semi-exclusive photon pair production and observation of exclusive and semi-exclusive electron pair production in pp collisions at $\sqrt{s} = 7$ TeV,” *JHEP* **1211**, 080 (2012) [arXiv:1209.1666 [hep-ex]].